# Laminar Boundary-Layer Control by Combined Blowing and Suction in the Presence of Surface Roughness

G. F. ANDERSON*
*Southeastern Massachusetts Technological Institute, North Dartmouth, Mass.*
V. S. MURTHY†
*Massachusetts Institute of Technology, Cambridge, Mass.*
AND
S. P. SUTERA‡
*Washington University, St. Louis, Mo.*

**The feasibility of maintaining a fully laminar boundary layer on a given two-dimensional body by combined blowing and suction is investigated theoretically and experimentally. Based on calculated potential flow past the body boundary layer, calculations are made for various blowing rates at the stagnation point. Experiments with a model designed for area suction and blowing indicate that the combination of suction to maintain a laminar boundary layer and blowing near the stagnation point to improve the tolerance of the laminar boundary layer to roughness can substantially reduce the skin friction of bodies at high Reynolds numbers.**

## Nomenclature§

$a$ = half-width of the body beyond the shoulder
$L$ = length of the body
$\bar{n}$ = distance normal to the surface of the body
$r$ = ratio of major to minor diameters for elliptical noses
$R_a$ = Reynolds number based on the half-width of the body and undisturbed freestream velocity = $\overline{U}_0 a/\nu$
$R_L$ = Reynolds number based on the length of the body and undisturbed freestream velocity = $\overline{U}_0 L/\nu$
$R_\theta$ = Reynolds number based on the momentum thickness and local freestream velocity = $\overline{U}\bar{\theta}/\nu$
$\bar{s}$ = distance along the surface measured from the stagnation point
$\overline{U}$ = tangential velocity at the outer edge of the boundary layer
$\overline{U}_0$ = velocity of the undisturbed freestream
$\overline{V}_w$ = velocity through the surface (positive outwards)
$\overline{V}_{w0}$ = blowing velocity at the stagnation point
$\bar{x}$ = distance along the axis, measured from the nose
$\bar{y}$ = distance perpendicular to the axis
$\overline{\delta}_1$ = measure of the boundary-layer thickness
$\overline{\delta}^*$ = displacement thickness = $\int_0^\infty \left(\frac{1-\bar{u}_s}{\overline{U}}\right) d\bar{n}$
$\epsilon$ = height of the roughness element
$\epsilon_{max}$ = maximum allowable roughness height for the boundary layer
$\epsilon_0$ = maximum allowable roughness height with no blowing at the stagnation point
$\epsilon_v$ = maximum allowable roughness height with blowing at the stagnation point
$\eta$ = $\bar{n}/\overline{\delta}_1$
$\bar{\theta}$ = momentum thickness of the boundary layer = $\int_0^\infty \frac{\bar{u}_s}{\overline{U}} \frac{1-\bar{u}_s}{\overline{U}} d\bar{n}$
$\nu$ = kinematic viscosity
$\bar{\rho}_0$ = density of the fluid
$\bar{\tau}_w$ = shear stress at the wall

Presented as Paper 68-641 at the AIAA 4th Propulsion Joint Specialist Conference, Cleveland, Ohio, June 10–14, 1968; submitted June 20, 1968; revision received November 18, 1968. This research was supported by the Ordnance Research Laboratory, Penn State University, under Subcontract R66-2300 to Brown University.

* Associate Dean, College of Engineering. Member AIAA.
† Research Associate, Department of Mechanical Engineering.
‡ Chairman, Department of Mechanical and Aerospace Engineering. Member AIAA.

§ All the coordinates and velocities without overbar are dimensionless. Here linear dimensions are referred to the half-width $a$ of the body and velocities to the undisturbed freestream velocity $\overline{U}_0$.

## 1. Introduction

THIS study concerns the reduction of skin friction on nonlifting, underwater vehicles. The technique proposed is that of laminar boundary-layer stabilization by means of distributed or area suction combined with blowing in the vicinity of the stagnation point to reduce the laminar layer's sensitivity to surface roughness. Although the technique is proposed specifically for a nonlifting, underwater vehicle at a length Reynolds number $Re_L$ beyond $10^6$, it should also be relevant for a lifting airfoil on which pressure drag is minimized.

Of the methods under investigation to reduce skin friction by alteration of the turbulent boundary layer[1] such as the addition of high molecular weight polymers (the Toms phenomenon), the maintenance of a laminar boundary layer offers the greatest potential drag reduction. With "optimum" suction, for example, the theoretical saving in drag relative to the fully turbulent drag ranges from 65% to 85% for a flat plate.[2]

Boundary-layer suction (BLS) can stabilize a laminar boundary layer to fluid-dynamic disturbances in the flow outside the boundary layer, due to the greater convexity (inward) of the velocity profile in the suction boundary layer. A considerable amount of analytical and experimental work has been recorded[2] on the application of BLS to lifting surfaces, mostly concerned with attainment of high lift-to-drag ratios where BLS delayed or prevented separation. On the other hand, little experimental work on laminarization of bodies of revolution has appeared in the open literature. In Lachmann[3] mention is made of experiments by Gregory and Walker[4] in which laminar flow was maintained over 82% of the body length at Reynolds numbers of nearly $10^7$. At higher speeds transition was said to be provoked by surface

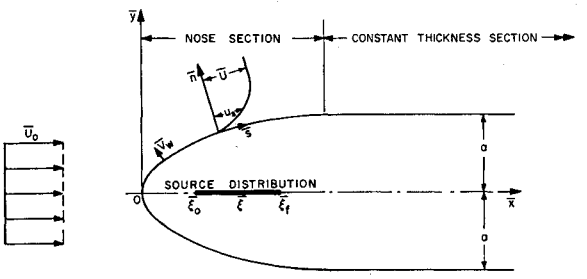


**Fig. 1 The coordinate system, source distribution, and body profile.**

discontinuities. More recently, Anderson and Sutera[5] reported wind-tunnel experiments on a slender body of revolution with a porous surface for area suction. They indicated that the limiting Reynolds number for effective maintenance of a laminar boundary layer by BLS depended on surface smoothness.

The role of roughness in this apparent Reynolds number limitation may be understood by considering how Reynolds number is increased in the usual wind- or water-tunnel experiment. As the model scale and fluid viscosity are fixed, $Re_L$ can only be increased by increasing the velocity of the freestream. However, this velocity increase reduces boundary-layer thickness everywhere on the body (approximately as $U_0^{-1/2}$ for a laminar layer). Consequently, the ratio of the height of any roughness element to the local boundary-layer thickness increases with Reynolds number, which causes a "tripping" transition of the laminar layer. This chain of events would not take place if the Reynolds number could be increased by elongating the body at constant $U_0$. The fact that roughness is important and that an appropriate dimensionless roughness parameter cannot be uncoupled from $Re_L$ in the constant-length model experiment may not have been fully recognized in recent (classified) investigations of BLS.

A main purpose of the present program is to emphasize the role of roughness in laminar boundary-layer control. This is done by first analyzing the maximum tolerable roughness distribution on a given body on whose surface an optimum suction distribution is maintained. An "optimum" suction distribution is one in which the minimum amount of suction necessary to prevent transition is applied at each point on the body. An increase in suction beyond the optimum decreases the boundary-layer thickness. This thinning action, while increasing the layer's stability to fluid-dynamic disturbances, has two undesirable effects. First, it increases the wall shear stress, thereby increasing over-all skin friction. Second, it gives greater prominence to surface defects and increases the boundary layer's vulnerability to tripping from within.

A second major purpose—the essential innovation in the proposed technique—is to evaluate, analytically and experimentally, the effectiveness of stagnation-point blowing in reducing the suction boundary layer's sensitivity to roughness. Stagnation-point blowing adds mass to the boundary layer and thickens it before it is exposed to suction, with no concomitant increase in local shear rate. Although injection of fluid normal to the wall is usually considered destabilizing, an analysis by Tetervin and Levine[6] indicates that, in a favorable pressure gradient, an increase in boundary-layer thickness by normal injection through the surface can result in a stable velocity profile. The present experiments show that relatively high blowing rates can be tolerated near the stagnation point without upsetting a laminar layer maintained by distributed suction.

## 2. Analysis

The objective of the analysis was to determine the effect of blowing in the stagnation region on the tolerable roughness height for a boundary layer maintained laminar by area suction on a particular two-dimensional body. This determination was preceded by the choice of a body profile and a complete calculation of its suction boundary layer for a range of stagnation blowing rates.

The choice of the body profile hinged on: 1) the pressure distribution on the body and 2) the practical constraints imposed by the internal compartments needed for variable blowing and suction. The requirements of 1) blunt nose, 2) continuous slope, and 3) weak adverse pressure gradient downstream of the minimum pressure point led to a choice of an elliptical nose joined at its minor diameter to a constant-thickness section, as shown in Fig. 1.

Calculated first was the potential flow about a symmetrical, two-dimensional, semi-infinite body (see Fig. 1), starting with a planar source distribution which closely approximates the actual body in a uniform flow. The velocity distribution on this "parent" body is then modified, using the techniques of slender-body theory, to obtain a more exact velocity distribution on the actual body. The calculation of the potential flow is detailed in Ref. 7.

Next, the velocity distribution on any chosen body is used to calculate the boundary layer with suction and blowing on that body, with the blowing rate at the stagnation point used as a parameter. For each value of the parameter, the blowing-suction distribution is determined according to the criterion of critical momentum-thickness Reynolds number for instability at every point, except in the narrow region that includes the stagnation point where the blowing rate is constant and the boundary layer subcritical. The boundary-layer calculation also yields the velocity-profile and skin-friction distributions.

Finally, the second, or roughness, criterion for transition is used to calculate the maximum roughness height that can be tolerated at each point on the body. Because the stagnation-blowing rate is a parameter in the boundary-layer calculation, the maximum roughness distribution is obtained as a function of that blowing rate.

### 2.1 Boundary-Layer Analysis

The objectives of the boundary-layer analysis are to determine 1) the velocity through the body surface required to maintain the laminar boundary layer on the verge of instability and 2) the effect of blowing on the boundary layer's tolerance to roughness.

The velocity profiles in the boundary layer are approximated by a one-parameter family,[9] which is a linear combination of the approximate Blasius and the asymptotic suction profiles;

$$\bar{u}_s/\overline{U} = F_1(\eta) + KF_2(\eta) \tag{1}$$

where

$$F_1(\eta) = 1 - e^{-\eta} \quad \text{(asymptotic suction profile)} \tag{2}$$

$$F_1(\eta) - F_2(\eta) = \sin(\pi\eta\, 6), \quad \text{for } 0 \leq \eta \leq 3$$
$$= 1, \quad \text{for } \eta \geq 3 \tag{3}$$

(approximate Blasius profile)

and $K$ is a coefficient which we will call the shape factor for this family of profiles. It is a function of position on the body surface.

Theoretically[6] the critical Reynolds number at which the boundary layer becomes unstable to fluid-dynamic disturbances is a function only of the shape of the velocity profile. In terms of the momentum-thickness Reynolds number, this criterion may be expressed as

$$R_{\theta c} = R_{\theta c}(K) \tag{4}$$

for the particular family of profiles. The function $R_{\theta c}(K)$ is

given in Fig. 1 of Ref. 6. For the boundary layer to remain laminar all along the body, $R_\theta$ must not exceed the particular value of $R_{\theta c}$ corresponding to the local shape of the velocity profile.

The calculation of the boundary-layer characteristics begins with the momentum-integral equation[9] generalized to include a velocity through the boundary $V_w$. In dimensionless form,

$$\frac{dR_\theta}{ds} = \frac{\bar{\tau}_w}{\bar{\rho}_0 \bar{U}^2} R_a U - \left(1 + \frac{\delta^*}{\theta}\frac{R_\theta}{U}\frac{dU}{ds} + V_w R_a\right) \quad (5)$$

The expressions for $\delta^*/\theta$, $\theta/\delta_1$, and $\bar{\tau}_w\bar{\theta}/\mu U$ in terms of the shape factor $K$ follow from the definitions of $F_1(\eta)$ and $F_2(\eta)$[9]:

$$\frac{\delta^*}{\theta} = \frac{1 - 0.09014K}{g(K)}, \quad \frac{\theta}{\delta_1} = g(K), \quad \frac{\bar{\tau}_w\bar{\theta}}{\mu\bar{U}} = g(K)[1 + 0.4764K] \quad (6)$$

where $g(K) = 0.5 + 0.6656K - 0.02348K^2$. It follows that

$$\bar{\tau}_w/\bar{\rho}_0\bar{U}^2 = \bar{\tau}_w\bar{\theta}/\mu\bar{U} \cdot (\nu/\bar{U}\bar{\theta}) = g(K)[1 + 0.4764K]1/R_\theta \quad (7)$$

Inserting (6) and (7) in the momentum-integral equation (5) we obtain a working form of one differential equation relating $R_\theta$, $K$, and $V_w$;

$$\frac{dR_\theta}{ds} = g(K)(1 + 0.4764K)\frac{R_a U}{R_\theta} - \left(1 + \frac{1 - 0.09014K}{g(K)}\right)\frac{R_\theta}{U}\frac{dU}{ds} + V_w R_a \quad (8)$$

A second relation is obtained by applying the boundary condition on the velocity profile[9] at the wall, i.e., at $\bar{n} = 0$,

$$\bar{V}_w \left.\frac{\partial \bar{u}_s}{\partial \bar{n}}\right|_{\bar{n}=0} = \bar{U}\frac{d\bar{U}}{d\bar{s}} + \nu \left.\frac{\partial^2 \bar{u}_s}{\partial \bar{n}^2}\right|_{\bar{n}=0} \quad (9)$$

Substitutions of expressions (1) and (6) for $\bar{u}_s$ and $\delta_1$ into Eq. (9) yields

$$\frac{g(K)(1 + K)}{R_\theta(1 + 0.4764K)} - \frac{R_\theta}{R_a U^2 g(K)(1 + 0.4764K)}\frac{dU}{ds} + \frac{V_w}{U} = 0 \quad (10)$$

Equations (8) and (10) include three unknowns, viz, $R_\theta(s)$, $V_w(s)$, and $K(s)$. At the stagnation point ($s = 0$), $R_\theta$ is always zero and hence the boundary layer can withstand any amount of blowing there. This has been established by Tetervin and Levine,[6] who also demonstrated that the velocity profile approaches a sine profile for large blowing velocities. For practical reasons, however, the blowing velocity $V_w$ is assigned a fixed positive value (blowing) in a region near the nose beginning at $s = 0$, and Eqs. (8) and (10) are then solved simultaneously for $R_\theta$ and $K$. In this domain the boundary layer is subcritical up to a point $s_c$ where $R_\theta(s_c)$ equals $R_{\theta c}[K(s_c)]$. From that point, calculations of the boundary-layer parameters to maintain a critical boundary layer are performed, viz.,

$$R_\theta(s) = R_{\theta c}[K(s)] \text{ for } s > s_c \quad (11)$$

This condition provides the third equation needed beyond $s = s_c$.

Integration of the momentum integral equation is carried out step by step. $R_\theta$ at $s + \Delta s$ is calculated in terms of known quantities at $s$ as follows: 1) A first approximation to $R_\theta$ at $s + \Delta s$ is

$$R^{(0)}_{\theta_{s+\Delta s}} = R_{\theta_s} + \left(\frac{dR_\theta}{ds}\right)_s \Delta s \quad (12)$$

2) This value of $R_{\theta_{s+\Delta s}}$ is used to calculate a first approximation to the derivative of $R_\theta$ at $s + \Delta s$ from Eq. (18) and an improved value of $R_{\theta_{s+\Delta s}}$ is determined by the formula

$$R^{(1)}_{\theta_{s+\Delta s}} = R_{\theta_s} + \frac{\Delta s}{2}\left[\left(\frac{dR_\theta}{ds}\right)_s + \left(\frac{dR_\theta}{ds}\right)^{(0)}_{s+\Delta s}\right] \quad (13)$$

3) Step 2 is reiterate using the value $R^{(1)}_{\theta_{s+\Delta s}}$ to obtain a third approximation $R^{(2)}_{\theta_{s+\Delta s}}$. 4) If the difference between $R^{(2)}_{\theta_{s+\Delta s}}$ and $R^{(1)}_{\theta_{s+\Delta s}}$ is within tolerance, then $R^{(2)}_{\theta_{s+\Delta s}}$ is taken to be the value of $R_\theta$ at $s + \Delta s$. Otherwise, the step length is reduced and the process repeated.

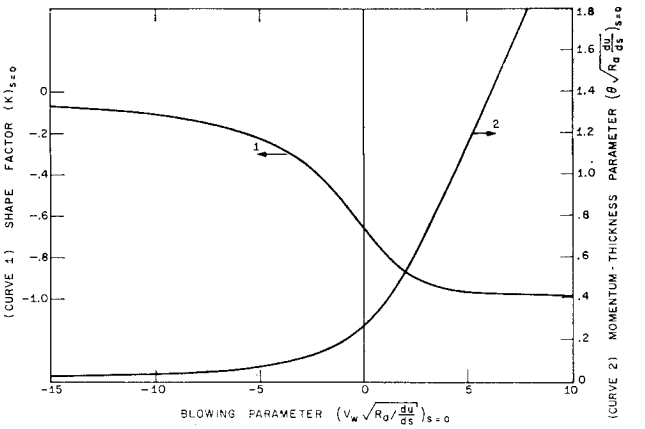


**Fig. 2 Boundary-layer parameters at the stagnation point.**

The computation must begin at a stagnation point, and hence the values of the momentum thickness $\theta$ and the shape factor $K$ have to be determined there for the specified blowing rate. For this purpose, we use the momentum-integral Eq. (8). From this equation, in order for the derivative $d\theta/ds$ to be finite at the stagnation point where $U = 0$, we must have

$$g(K)(1 + 0.4764K)\frac{1}{R_a\theta} - \left[2 + \frac{1 - 0.09014K}{g(K)}\right]\theta\frac{dU}{ds} + V_w = 0 \quad \text{at } s = 0 \quad (14)$$

This equation and Eq. (10) are solved simultaneously to give $K$ and $\theta$ at $s = 0$. $K$ at $s = 0$ is then obtained from

$$\frac{(1 + 0.4764K) - (1 + K)[2g(K) + 1 - 0.09014K]}{\{g_1(K)[(1 + 0.4764K)^2 - (1 + K)]\}^{1/2}} = V_w\left(\frac{R_a}{dU/ds}\right)^{1/2} \text{ at } s = 0 \quad (15)$$

where $g_1(K) = 2g(K)(1 + 0.4764K) + (1 - 0.09014K) \times (1 + 0.4764K) - 1$. The quantity $\{V_w[R_a/(dU/ds)]^{1/2}\}_{s=0}$ will be referred to as the blowing parameter. The momentum-thickness parameter, $\{\theta[R_a(dU/ds)]^{1/2}\}_{s=0}$ is calculated with the aid of Eqs. (10) and (14);

$$\{\theta[R_a(dU/ds)^{1/2}]\}_{s=0} = g(K)\{[(1 + 0.4764K)^2 - (1 + K)]/g_1(K)\}^{1/2} \text{ at } s = 0 \quad (16)$$

Insertion of the assigned value of $V_{w0}$ and the known values of $R_a$ and $dU/ds|_{s=0}$, which is obtained from the potential flowfield, into Eq. (15) determines $K$ at $s = 0$. Solution for $K(s = 0)$ is performed graphically with the aid of Fig. 2, where $K$ is plotted as a function of the blowing parameter. Also in Fig. 2, the momentum-thickness parameter is plotted as a function of the blowing parameter determined by means of Eqs. (15) and (16). Hence, the momentum thickness at $s = 0$ can be obtained directly when $K(s = 0)$ is known.

With all the necessary quantities now determined at $s = 0$, L'Hospital's Rule can be applied to get the value of $d\theta/ds$ at $s = 0$, using Eqs. (8) and (10). Complete results can be seen

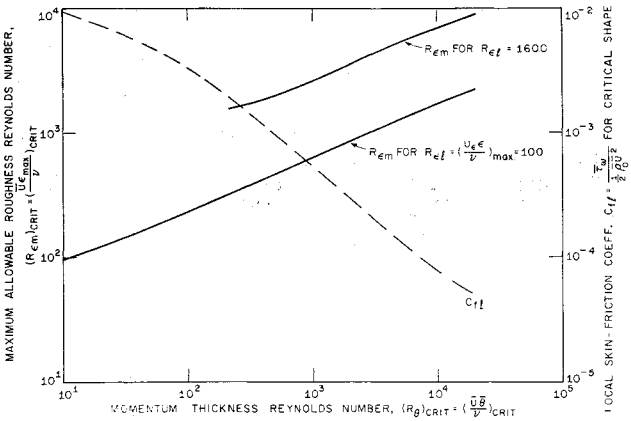


**Fig. 3 Maximum allowable roughness Reynolds number and local skin-friction coefficient vs momentum-thickness Reynolds number corresponding to critical conditions.**

in Ref. 7, p. 29. Subsequently, the conditions that $d^2U/ds^2 = 0$ at the stagnation point (symmetrical, blunt-nosed body) and $dV_w/ds = 0$ ($V_w$ maintained constant near $s = 0$) are applied with the result that $d\theta/ds$ must vanish at the stagnation point. With the initial values of $\theta$ and $d\theta/ds$ determined, the stepwise procedure outlined earlier may now be undertaken.

### 2.2 Skin Friction

The local skin-friction coefficient is defined as

$$C_{fl}(s) = \bar{\tau}_w / \tfrac{1}{2}\bar{\rho}_0 \overline{U}^2 \tag{17}$$

Substituting

$$\bar{\tau}_w = \mu \left.\frac{\partial \bar{u}_s}{\partial \bar{n}}\right|_{\text{wall}}$$

and using Eqs. (1) and (6) to express the velocity gradient at the wall in terms of $K$ and the momentum-thickness Reynolds number $R_\theta$,

$$C_{fl}(s) = 2g(K)(1 + 0.4764K)/R_\theta \tag{18}$$

For a boundary layer maintained in the critical condition, $R_\theta (= R_{\theta c})$ is a unique function of $K$ and conversely; hence, $C_{fl}$, as expressed by Eq. (18), can be represented as a function of $R_\theta$ alone for the critical profile, as displayed by Fig. 3.

The total skin-friction coefficient $C_{ft}$ is obtained by integrating over the body surface from the stagnation point to any axial station $x$. For one side of the body only and per unit span,

$$C_{ft} = \frac{1}{x}\int_0^x C_{fl}(\overline{U}/\overline{U}_0)^2\, dx' \tag{19}$$

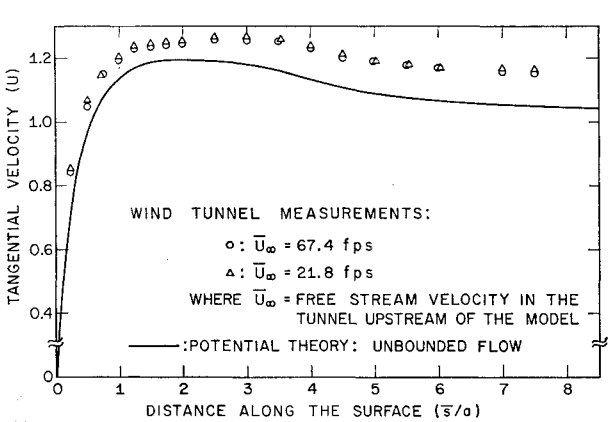


**Fig. 4 Velocity distribution on the model; $r$ = 4:1.**

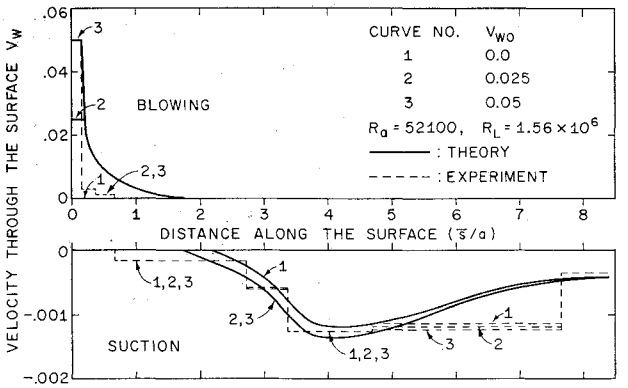


**Fig. 5 Velocity through the body surface; $r$ = 4:1 (note change of scale between blowing and suction).**

### 2.3 Maximum Allowable Roughness Height

Once the momentum-thickness Reynolds number and the shape factor are known, the maximum allowable roughness height may be calculated using the second stability criterion, which is given in terms of a Reynolds number $R_\epsilon$ based on the roughness height $\epsilon$ and the velocity $\overline{U}_\epsilon$ at the top of the roughness element[3]

$$R_{\epsilon l} = (\overline{U}_\epsilon \epsilon/\nu)_{\max} = 100 \text{ to } 1600 \tag{20}$$

The range for $R_{\epsilon l}$ reflects the fact that the tolerable value depends on the geometry of the roughness, i.e., the shape of the individual elements and their relative arrangements.

The maximum allowable roughness height at any given point on the body surface may be expressed in terms of a Reynolds number,

$$R_{\epsilon m} = \overline{U}\epsilon_{\max}/\nu \tag{21}$$

The velocity at the top of the roughness element may be obtained by putting $\bar{n} = \epsilon$ in Eq. (1). Inserting the result into Eq. (20) for maximum allowable roughness height and using Eq. (21), we obtain

$$R_{\epsilon l} = R_{\epsilon m}(1 - \exp\{-g(K)R_{\epsilon m}/R_\theta\} + K[1 - \exp\{-g(K)R_{\epsilon m}/R_\theta\} - \sin\{\pi g(K)R_{\epsilon m}/(6R_\theta)\}]) \tag{22}$$

which may be solved for $R_{\epsilon m}$ for any given $R_{\epsilon l}$.

Since $R_\theta (= R_{\theta c})$ is a unique function of $K$, $R_{\epsilon m}$, as given by Eq. (22) for any given value of $R_{\epsilon l}$, may be considered a function of $R_\theta$ alone for the critical profile. This is displayed in Fig. 3 for $R_{\epsilon l}$ = 100 and 1600.

### 2.4 Computations

The numerical computations are in two main phases:

1) Freestream velocity distributions on bodies with elliptical noses. Results are summarized in Fig. 6 of Ref. 7. The solid

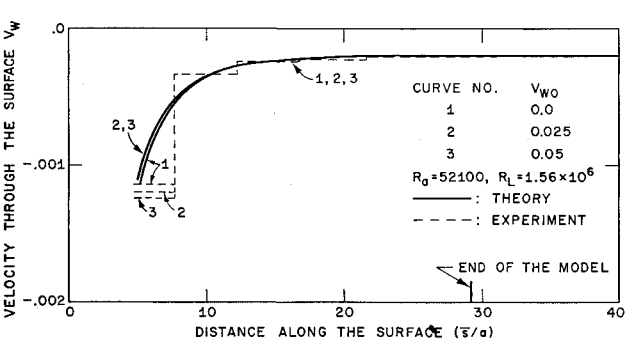


**Fig. 6 Velocity through the body surface; $r$ = 4:1.**

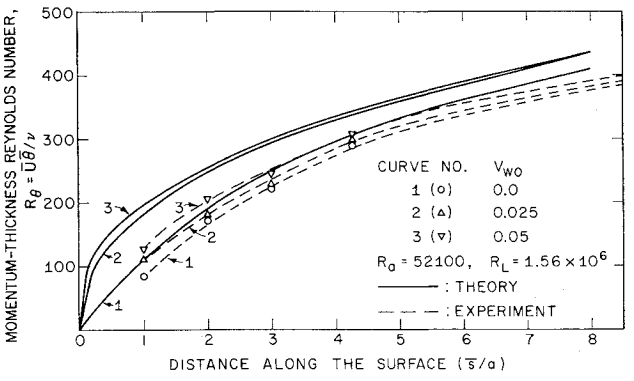


**Fig. 7 Momentum-thickness Reynolds number along the body surface; forward section $r$ = 4:1.**

curve in Fig. 4 represents the numerical computations for the 4:1 elliptical nose and unbounded freestream.

2) The second phase was concerned with boundary-layer parameters, based on the formulas developed in Secs. 2.1, 2.2, and 2.3. The boundary-layer parameters along the surface of the 4:1 body for various blowing rates are given by the solid curves in Figs. 5–10. The relative gain in the maximum allowable roughness height with blowing is presented in Fig. 11, and the total skin friction in Fig. 12. The complete set of computations is displayed in Figs. 9–16 of Ref. 7.

## 3. Experiment

### 3.1 Apparatus

For the experimental investigation, a model with a porous surface was used. Within a framework of brass ribs and spars, internally isolated compartments were provided in order to apply different rates of blowing or suction at the outer surface. A schematic diagram of the model compartments and dimensions of the segments is given in Fig. 13. The model is essentially divided into three spanwise sections, two end sections or guard sections each 5 in. wide, and a central test section 12 in. wide. The guard sections control the two-dimensionality of the flow over the test section by reducing the effect of the wind-tunnel walls between which the model is supported.

The model frame consists of thick brass ribs and spars joined in a grid-like arrangement. Brass tubes inserted through the side ribs feed the individual compartments in both the test and the guard sections of all the compartments in order to measure respective pressures. The complete framework of ribs and spars and the compartment walls were covered with perforated brass sheet, which was then covered with successive layers of dacron sail cloth, stainless-steel twill wire cloth (AISI Type 316, 0.007-in.-diam wire), and stainless-steel calendered wire cloth (AISI Type 316, 0.0014-in.-diam wire). The innermost layer of perforated brass sheet stiffens the

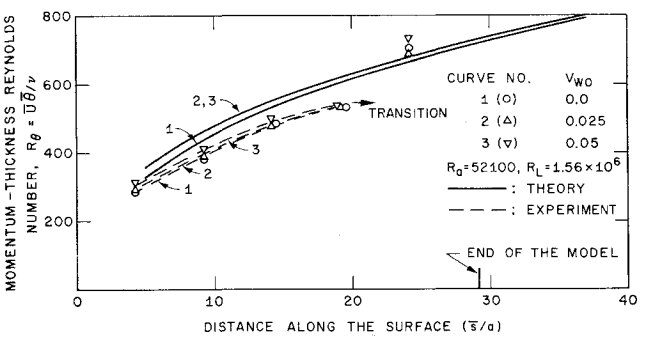


**Fig. 8 Momentum-thickness Reynolds number along the body surface; aft section $r$ = 4:1.**

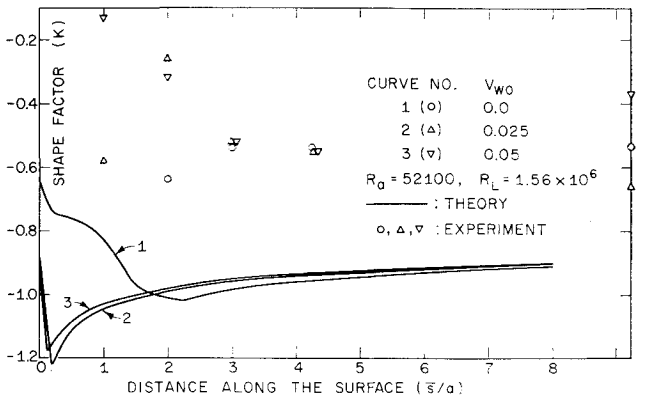


**Fig. 9 Shape factor along the body surface; forward region $r$ = 4:1.**

model and provides a solid base for the outer porous layers. The dacron cloth is a high resistance barrier and inhibits variations of suction or injection flux over an individual compartment that might be caused by the static-pressure gradient along the surface. The layer of stainless-steel cloth minimizes the distributed jet-like character of the flow at the perforated sheet. The outermost layer of calendered stainless-steel cloth provides a smooth porous surface for the outer flow.

The flow through the skin is delivered to the suction and blowing manifolds through valves and calibrated porous plug flow meters. A few chambers are connected to both manifolds to permit either suction or blowing. Static-pressure tubes from the test and the guard sections are connected to a bank of U-tubes so that the pressures in the individual test or guard sections may be equalized to ensure spanwise uniformity of the flow through the surface.

The model is placed symmetrically in a subsonic closed-circuit, closed-jet wind tunnel with a test section 32 × 22 in. To measure the boundary-layer velocity profiles, two flat total-head tubes are employed, depending on the boundary-layer thickness. One tube has a tip 0.01 in. thick on the outside with an opening 0.0035 in. wide, and is used for boundary layers less than 0.15 in. in thickness. The tip of the other probe is 0.016 in. thick on the outside with a 0.006-in. opening. Whether the flow is laminar or turbulent is detected by a constant temperature hot-wire anemometer.

### 3.2 Wind-Tunnel Blockage Effect

The presence of the model in the test section results in a total-flow blockage, which may be expressed[10] as an average change in freestream velocity $u_1$, and is a function of body shape and length, jet area, and maximum body frontal area. For the two-dimensional body the closed tunnel data at velocity $V$ compare with free air data at velocity $V + u_1$, where the velocity increment $u_1$ is given by the empirical

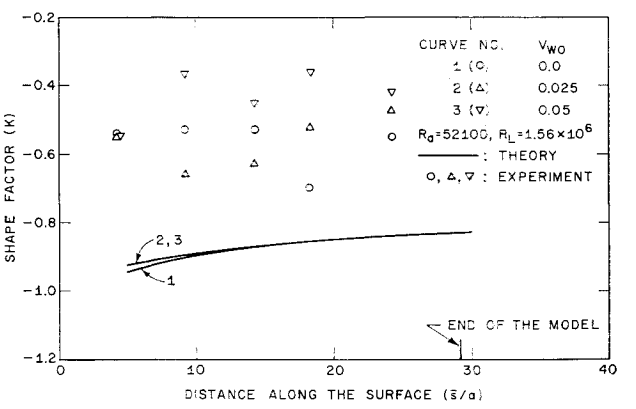


**Fig. 10 Shape factor along the body surface; aft section $r$ = 4:1.**

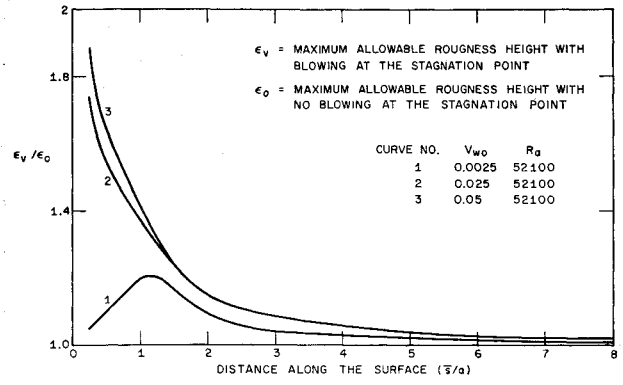


**Fig. 11 Gain in the maximum allowable roughness height due to blowing; $r = 4{:}1$. Limiting roughness Reynolds number, $R_{\epsilon l} = U_\epsilon \epsilon/\nu_{\max} = 100$.**

formula[10]

$$u_1/V = 0.32 \text{ vol}/(h^2 b)$$

where vol. = model volume = 5100 in.$^3$, $b$ = length of the side of the tunnel parallel to the model span = 22 in., $h$ = length of the other side of the tunnel = 32 in.

For the experiment,

$$u_1/V = 0.14$$

Thus, wind-tunnel data at a velocity $V$ correspond to free-air data at 1.14 $V$. This relation is used in comparing the theoretical and measured values.

### 3.3 Procedure

The static pressure on the model surface was measured at two different tunnel velocities by a static pressure probe, and the local freestream velocities are calculated from these measurements.

All the boundary-layer data were obtained at a tunnel speed such that the equivalent free air velocity, accounting for the blockage effect, is equal to 50 fps, which is one of the velocities for which the theoretical computations were made. An approximate blowing-suction distribution was established on the model and the boundary layer at the end of the model tested for turbulence by the hot-wire anemometer. Necessary adjustments were made to the blowing-suction distribution in order that 1) transition would occur slightly upstream of the end of the model, and 2) any significant change in the flow through any compartment would change the location of the transition point. The transition point is here defined as the location at which approximately equal intervals of laminar and turbulent flow are observed. After adjusting the blowing-

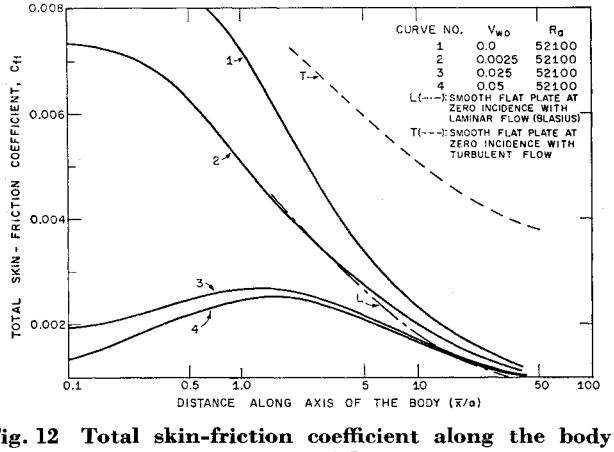


**Fig. 12 Total skin-friction coefficient along the body; $r = 4{:}1$.**

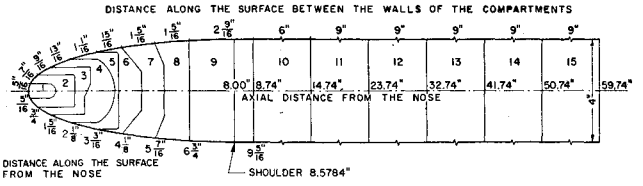


**Fig. 13 Schematic diagram of model compartments (not to scale).**

suction distribution, boundary-layer velocity profile measurements were made 2, 4, 6, 8.58, 18.58, 28.58, 36.58, and 48.58 in. downstream of the stagnation point along the surface. The momentum-thickness Reynolds numbers and the shape factors for the measured boundary-layer profiles were calculated by finding the curves which belonged to the one-parameter family of Eq. (6) and which, at the same time, were optimum fits to the measured profiles.

The guard sections were only partly effective in establishing a perfectly two-dimensional flow along the full length of the test section of the model. The flow in the midspan plane, however, could easily be maintained laminar and hence measurements were made in that plane.

### 3.4 Results

The measured local freestream velocity distribution on the model is displayed in Fig. 4 along with the theoretical distribution for unbounded flow. The blowing-suction distribution is portrayed in Figs. 5 and 6. Figure 5 has portions for blowing and for suction. Measured and theoretical distributions of momentum-thickness Reynolds numbers are depicted in Figs. 7 and 8. Finally, the comparison between theory and experiment with regard to shape factor is given in Figs. 9 and 10.

## 4. Discussion of Results and Conclusions

The analysis indicates that substantial benefits can be realized by blowing near the stagnation point. It predicts that the relative increase in the boundary-layer thickness decreases as the blowing rate increases, and even small blowing velocities (of the order of 1% of the undisturbed freestream velocity) considerably thicken the boundary layer. The theoretical improvement in tolerance to roughness (Fig. 11) is substantial. The predicted increase in the maximum allowable roughness height diminishes at large distances from the stagnation point. However, since the boundary layer in this region is normally thick enough to tolerate large roughness heights, artificial thickening is less important.

Most of the theoretical predictions were borne out by the experiments. The significant discrepancy between the theoretical calculations, which are exact for unbounded flow, and the measured distribution of local freestream velocity at the surface of the body, as seen in Fig. 4, is due to the blockage effect. Far downstream of the shoulder the local freestream velocity on the model is about 14% higher than predicted by the theory.

As seen from Figs. 5 and 6, the suction distribution required to maintain laminar flow over the model compares favorably with the theoretical distribution for an unbounded flow. In contrast, the blowing could not be extended as far downstream of the stagnation point as predicted by analysis. This is explained by the fact that the favorable pressure gradient does not extend as far from the nose of the model in the wind tunnel as it does in theory, thus restricting the area where blowing is allowable.

Measured and theoretical distributions of the momentum-thickness Reynolds number and of the shape factor are shown in Figs. 7 to 10. They agree fairly well, considering that the pressure distribution and the blowing-suction distribution on the model are not the same as those used in the theory. The

restriction of the extent of blowing, and the step-wise character of the blowing-suction distribution which necessitates less blowing and more suction than the optimum distribution, reduce the momentum-thickness Reynolds number and bring the boundary-layer velocity profiles closer to the asymptotic suction profile ($K = 0$). The change in profile results in a larger shape factor for the measured velocity profiles.

The results of Figs. 5–10 correspond to transition about 5 in. upstream of the end of the model. Any attempt to establish transition at the very end of the model would be confused by disturbances of the wake of the model. For convenience in detecting the nature of the boundary-layer flow, the transition point, rather than fully laminar flow, was established at the chosen location. Judgment of a fully laminar flow, just devoid of turbulence, involves the risk of establishing a subcritical laminar boundary layer.

The combination of suction applied to maintain a laminar boundary layer and blowing at the stagnation point to improve the tolerance of the boundary layer to roughness should be ideal for substantially reducing skin friction of bodies at high Reynolds numbers.

With an appropriate choice of the blowing rate, the fluid removed by suction may be the same fluid injected near the stagnation point. For example, for a body with a 4:1 elliptical-nose and a length-to-thickness ratio of 15, the amounts of the injected and the sucked fluid are equal for a blowing rate of 1.2% at the stagnation point. This procedure would reduce the danger of clogging the porous skin in flights through turbid fluids, since most of the sucked fluid is composed of the fluid ejected at the nose, and eliminate the necessity of disposing of the sucked fluid.

## References


[1] Lumley, J. L., "The Reduction of Skin-Friction Drag," ACR-112, 1964, Office of Naval Research, Department. of the Navy, Washington, D.C. p. 915.

[2] Schlichting, H., *Boundary Layer Theory*, 4th ed., transl. by J. Kestin, McGraw-Hill, New York, 1960.

[3] Lachmann, G. V., *Boundary Layer and Flow Control*, Pergamon Press, New York, 1961.

[4] Gregory, N. and Walker, W. S., "Wind Tunnel Tests on the Use of Distributed Suction for Maintaining Laminar Flow on a Body of Revolution," ARC 19, July 1957, pp. 4–28, Office of Naval Research, Washington, D.C.

[5] Anderson, G. F. and Sutera, S. P., "Drag Reduction of Bodies of Revolution by Use of Area Suction," *AIAA Journal*, Vol. 3, No. 10, Oct. 1965, pp. 1970–1972.

[6] Tetervin, N. and Levine, D. A., "A Study of the Stability of the Laminar Boundary Layer as Affected by Changes in the Boundary-Layer Thickness in Regions of Pressure Gradient and Flow through the Surface," TN 2752, Aug. 1952, NACA.

[7] Anderson, G. F., Sutera, S. P., and Murthy, V. S., "Laminar Boundary Layer Control by Combined Blowing and Suctions in the Presence of Roughness," Rept. WT-51, Oct. 1967, Brown University.

[8] Sutera, S. P., Murthy, V. S., and Anderson, G. F., "Laminar Boundary Layer Control by Combined Blowing and Suction in the Presence of Roughness," Paper 68-641, 1968, AIAA.

[9] Schlichting, H., "An Approximate Method for the Calculation of Laminar Boundary Layer with Suction for Bodies of Arbitrary Shape," TN 1216, March 1949, NACA.

[10] Pope, A., *Wind Tunnel Testing*, Wiley, New York, 1947.


# Engineering Notes

*ENGINEERING NOTES are short manuscripts describing new developments or important results of a preliminary nature. These Notes cannot exceed 6 manuscript pages and 3 figures; a page of text may be substituted for a figure and vice versa. After informal review by the editors, they may be published within a few months of the date of receipt. Style requirements are the same as for regular contributions (see inside back cover).*

## Similar Solutions of the Boundary-Layer Equations for a Non-Newtonian Fluid


E. R. Thompson*

*Arnold Engineering Development Center, Arnold Air Force Station, Tenn.*


### Nomenclature

$c_p$ = constant pressure specific heat
$k$ = thermal conductivity
$K,N$ = constants in the power-law shear model
$r$ = constant in Ref. 7 describing the required temperature distribution for similar solutions
$T$ = temperature
$u,v$ = velocity in the $x$ and $y$ direction, respectively
$\rho$ = density

*Subscripts*

$L$ = characteristic or reference length
$\infty$ = reference (freestream) conditions
$w$ = wall conditions

Received October 9, 1968.

* Aerodynamicist, Advanced Plans Division of the Directorate of Plans and Technology.

### Introduction

THE mathematical simplifications to the boundary-layer equations which are possible when the concept of similar solutions is utilized are well known from classical Newtonian flow[1,2] and will not be reiterated in this note. Schowalter[3] and Acrivos, Shah, and Petersen[4] were among the first to publish the results of investigations of the flow of a non-Newtonian fluid past an external surface. Schowalter's primary objective was to determine those flows of a power-law non-Newtonian fluid for which similar solutions could be obtained for the momentum equation. Acrivos et al. obtained numerical solutions of the momentum equation for the flow of the same type of fluid past a horizontal flat plate. The heat-transfer coefficient was also obtained by considering an asymptotic form of the energy equation valid in the limiting case of large Prandtl numbers.

Among the investigators that have considered the subject of similar solutions of the boundary-layer equations for external flow of non-Newtonian fluids since the investigations of Schowalter and Acrivos, Shah, and Petersen are the authors of Refs. 5–7. Only in the papers by Acrivos et al.[4] and Lee and Ames[7] was the energy equation considered in the investigation to determine the possibility of obtaining similar solutions. The authors of the former paper concluded that similar solutions did not exist for the energy equation for the case of the